

Experimental Implementation of Neural Network Springback Control for Sheet Metal Forming

Vikram Viswanathan

Department of Mechanical Engineering,
Northwestern University,
Evanston, IL 60201

Brad Kinsey

Department of Mechanical Engineering,
University of New Hampshire,
Durham, NH 03824

Jian Cao

Assoc. Mem.
Department of Mechanical Engineering,
Northwestern University,
Evanston, IL 60201

The forming of sheet metal into a desired and functional shape is a process, which requires an understanding of materials, mechanics, and manufacturing principles. Furthermore, producing consistent sheet metal components is challenging due to the nonlinear interactions of various material and process parameters. One of the major causes for the fabrication of inconsistent sheet metal parts is springback, the elastic strain recovery in the material after the tooling is removed. In this paper, springback of a steel channel forming process is controlled using an artificial neural network and a stepped binder force trajectory. Punch trajectory, which reflects variations in material properties, thickness and friction condition, was used as the key control parameter in the neural network. Consistent springback angles were obtained in experiments using this control scheme. [DOI: 10.1115/1.1555652]

Introduction

The Partnership for a New Generation of Vehicles (PNGV), a wing of the United States Council for Automotive Research (USCAR), identified sixteen manufacturing technologies that need to be addressed in order to improve automotive manufacturing [1]. The “springback challenge,” i.e., finding a way to compensate and control springback, is one of these crucial manufacturing areas. Inconsistencies in part dimensions caused by springback increase changeover time and slow product launches. During a sheet metal forming, in particular the bending process, the region around the neutral plane in the material undergoes both elastic and plastic deformation. When the punch has reached the final draw depth and is removed, the elastic strain in the material is recovered, which produces springback in the part due to the nonuniform stress distribution in the sheet. Therefore, the final part configuration after unloading is different than the one in the loaded state as shown in the two dimensional channel part view of Fig. 1.

Efforts have been made to reduce the amount of springback in formed parts and to compensate for the amount of the springback in the tooling design [2,3]. From a quality control standpoint, consistent springback is critical to the following assembly processes. Factors that affect springback include variations in both material and process parameters [4–15], such as material properties, sheet thickness, friction condition, binder force, and tooling geometry, etc. The relationships that exist between springback and these parameters are extremely nonlinear with multiple interactions.

In order to address the unavoidable variations in material and process parameters that lead to inconsistent springback, modifications to the forming process have been proposed. Sunseri et al. [16] proposed a closed-loop control process to overcome variations in the friction conditions during a channel forming process. The binder force was adjusted to follow the desired punch force trajectory obtained from the stepped binder force at the nominal process conditions. Their work produced consistent springback levels when the friction coefficient was varied. However, the method was not tested for variations in other parameters such as material properties or thickness. Thickness variation was considered in Elkins and Sturges [17] where thickness and material hardness were measured prior to a small radius air bending operation.

These data were then used in an analytical model to calculate the punch depth to obtain desired springback angles. The methodology, which combined a model-based approach and on-line closed loop control, provided good springback control within 0.25 deg. However, this approach is only suitable for small volume production due to the time and cost associated with measuring the thickness and material hardness.

A promising alternative control system in metal forming processes is neural network control. The concept of neural network control and potential applications were discussed in Kinsey et al. [18]. Metal forming examples that have benefited from neural network springback control include a rebar [19] and an air bending process [20]. The inputs to the neural network in Inamdar et al. [20] included the ratio of yield strength to Young’s modulus and the strain hardening exponent, n . The network provided good springback predictions if the material parameters were accurate. Kim and Kim [21] reduced the number of finite element simulations necessary to design the die geometry for a cylindrical pulley and the initial billet size for an axisymmetric rib-web product using neural networks. In yet another research project, Manabe et al. [22] utilized a neural network to determine the material properties early in the forming process of a cylindrical part. Closed-loop control of the binder force was then employed based on the theoretical wrinkle limit in the initial forming depth stage of the process and the theoretical fracture limit in the latter forming depth stage. These theoretical limits were based on an analytical calculation using the material properties computed by the neural network and a friction coefficient, which was determined throughout the forming process.

Ruffini and Cao [23] and Kinsey et al. [18] proposed a control system using artificial neural networks and a stepped binder force trajectory to minimize and control springback in an aluminum

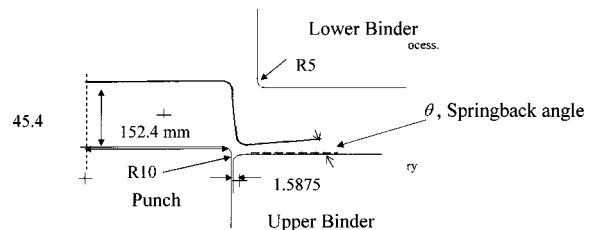


Fig. 1 Tooling geometry and springback angle in a plane strain channel forming

Contributed by the Materials Division for publication in the JOURNAL OF ENGINEERING MATERIALS AND TECHNOLOGY. Manuscript received by the Materials Division April 10, 2000; revision received April 11, 2001. Associate Editor: N. Chandra.

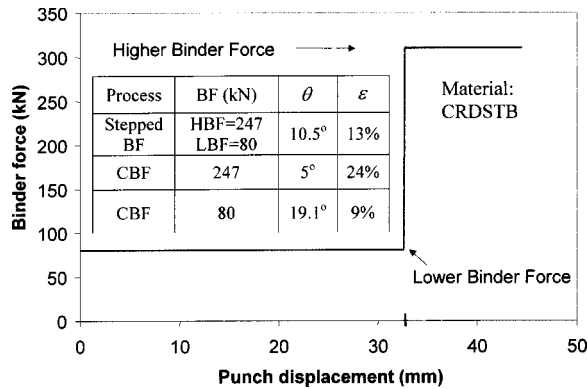


Fig. 2 A stepped binder force trajectory used in the channel forming process and its springback compared to constant binder force (CBF) cases

channel forming process. In these works, an artificial neural network was trained and implemented using numerical simulations results. A stepped binder force trajectory was known to produce a significantly lower amount of springback while keeping the strain level in the sheet at a reasonable value (see table in Fig. 2). However, the process variables related to a stepped binder force trajectory, the High Binder Force (HBF) value and the percentage of Punch Displacement (PD%) where the step in binder force occurs, needed to be adjusted based on variations in material and process parameters. A neural network was employed to determine these stepped binder force variables based on data from the initial forming of channels. A flowchart for the control scheme is shown in Fig. 3. In Kinsey et al. [18], four polynomial coefficients from the curve fitting of the punch force trajectory were used as inputs to the neural network. Based on these inputs, the neural network calculated the magnitude of the HBF and the PD% for the stepped binder force trajectory. Variations in the material properties were simulated by changing the material strength coefficient, K , and strain hardening exponent, n . Friction was varied by $\pm 65\%$, and sheet thickness was varied by $\pm 25\%$ compared to nominal values. Despite these large variations in process parameters, the neural network and stepped binder force trajectory maintained springback angles between 0.2 deg to 0.6 deg and the maximum strain values between 8% to 10%. This system provided an extremely robust control process at a low cost. Although the work was done using simulations, the results were promising. However, physical implementation of the process needed to be realized to verify the benefits.

In this paper, experimental results based on the method proposed by Kinsey et al. [18] are presented. Here, a steel channel forming process is used with a different geometry based on the tooling available. The punch force trajectory was again utilized to provide information about the material and process parameters for the inputs into the neural network with the outputs being variables for the stepped binder force trajectory, HBF and PD%. Details of

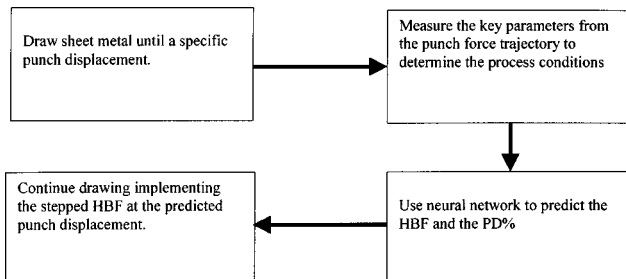


Fig. 3 Flow chart for implementing neural network control

numerical simulations that aided in the determination of experimental setups, specifics of neural network training, and the experimental results are presented. Consistent springback angle results were obtained even when materials not used in the neural network training process were formed.

Numerical Simulations

Finite element simulations were used to determine the experimental set up for our physical channel forming process. These analyses were performed on a commercial finite element package, ABAQUS/Standard [24]. The problem was approximated as a plane-strain condition, and the simulation was performed on one half of the length of the blank to take advantage of the symmetric in the geometry. The width of the blank in the simulation was also scaled down to one sixtieth of the experimental sample. The dimensions for the tooling were determined based on an existing pan forming tooling provided by ALCOA (see Fig. 1). The binder, die and punch were modelled as three rigid surfaces using four-node interface elements (ABAQUS type IRS4), and a Coulomb's friction law was assumed. The blank was meshed with two layers for a total of 200 eight-node elements with reduced integration (ABAQUS type CPE8R). The material was assumed to be planar isotropic following Hill's 1948 yield criterion and an isotropic hardening law was used. Further details can be found in Viswanathan [25].

Simulations were conducted to study the effects of binder force and forming depth on springback angle. The springback angle was found to increase with a deeper forming depth (Fig. 4) and a lower binder force (Fig. 5). The recoverable elastic strain would have a more inhomogeneous distribution through the thickness direction when a lower binder force is employed, and more sheet area will

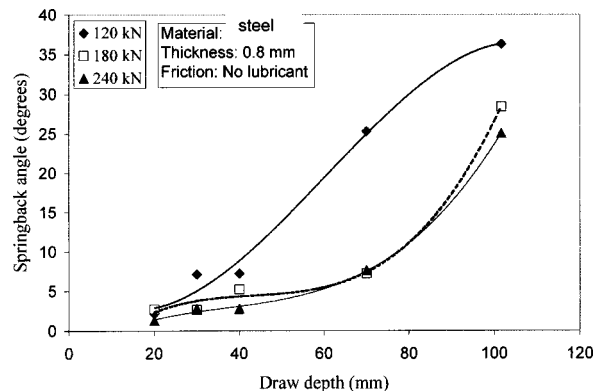


Fig. 4 Effect of drawing depth on springback angle at various constant binder forces

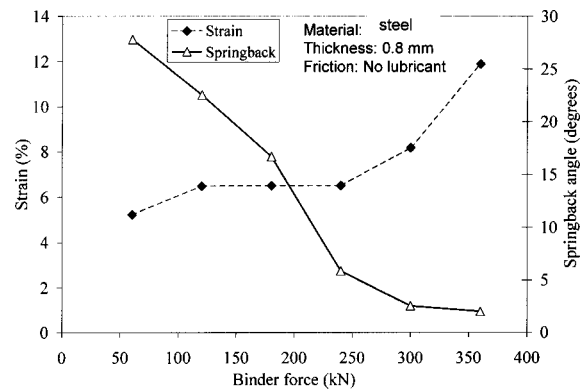


Fig. 5 Springback angle and maximum strain versus constant binder force

Table 1 Mechanical Properties* of Test Steels

Steel	Thickness (mm)	Yield** (MPa)	Ultimate tensile (MPa)	Maximum elongation (%)	<i>n</i>	K (MPa)	\bar{R}
CRDSTB	0.7366	155.60	301.6	39.5	0.239	536.47	1.51
EGCR3	0.7493	177.76	302.5	43.0	0.221	517.34	1.75
EGCR3-2	0.8509	165.36	291.5	44.6	0.224		1.901
HDGCR3	0.8001	194.20	354.3	37.5	0.220	623.50	1.46
HSGS25S	0.7620	187.60	306.5	40.1	0.225	537.70	1.57
EG250B	0.7542	249.98	360.5	33.2	0.179	574.70	1.64
Generic Steel	0.7014	Unknown	Unknown	Unknown	Unknown	Unknown	Unknown

*All properties are averaged according to $X = (2X_{45deg} + X_{0deg} + X_{90deg})/4$
 **Yield strength at 0.2% offset
 **Poisson's ratio is 0.3.

experience this uneven distribution at a deeper forming depth of this channel forming. Both of these causes result in more springback.

Experimental Setup

Numerical simulations conducted in the previous section provided guidance for the experimental setup, such as draw depth and blank width. Blanks of dimensions, 609.6 mm × 127 mm, were sheared from sheet metal provided by U.S. Steel Inc., with the rolling direction along the length of the blank. The cold-rolled materials used consisted of an electro-galvanized draw quality special killed steel of two different thickness (EGCR3, EGCR3-2), a hot dipped galvanized draw quality special killed steel (HDGCR3), a carbon sheet Chrysler Spec MS-steel (MS-67) (CRDSTB), an electro-galvanized-annealed high strength steel (HSGS25S) fully stabilized with a minimum yield strength of 172.4 MPa. Two additional steels used for verification, i.e. not seen by the neural network during training, are EG250B and a generic carbon steel. Material properties and thickness data are given in Table 1 for these materials. The value differences between these steels are 20% in K, 27% in *n*, and 14% in thickness; thus representing a significant range in material properties.

These blanks were then circle gridded using electrochemical etching to allow for strain measurements. Three different lubricants widely employed in the metal forming industry, a mineral oil, a pre lubricant and a synthetic coating, were used to generate various friction conditions. Typical coefficients of friction values for these lubricants vary from 0.05 to 0.15. This represents a 200% variation in the lubricating conditions. To produce the desired friction condition, 10 ml. of the appropriate lubricant was sprayed on the blank and distributed evenly on the surface. Blanks were also formed in the dry condition (approximately $\mu = 0.20$), which provides a total of four different lubrication conditions.

Experiments were performed on a 150-ton HPM hydraulic, double action stamping press. The pressures in four hydraulic cylinders, one in each corner of the binder plate, generate the binder force in the process and are controlled by proportional valves. A Temposonics displacement sensor monitors the punch position to determine the location to apply the stepped binder force trajectory. Labview, a graphical programming language, and data acquisition boards from National Instruments were used to output voltages to the proportional valves to control the binder force and to monitor the punch displacement, punch force, and binder force in the process. The channel was drawn to a depth of 44.5 mm, and the low binder force was a constant for all experiments, 80 kN. The springback angle was measured using a Coordinate Measuring Machine (CMM) after the process was completed.

Control System

Neural Networks. Neural networks are non-linear analysis tools that form a highly interconnected, parallel computation structure with several simple processing elements, or neurons.

Each neuron is linked to adjust, downstream neurons through variable weights. These weights are calculated by an iterative method during the training process when the network is fed with a large amount of training data, input and output pairs that represent the pattern attempting to be modeled. Neural networks have found diverse applications, for instance in speech generation [26], welding [27], and medical diagnosis [28].

Hornik et al. [29] showed that a two-layer neural network, one made up of an input layer, a hidden layer, and an output layer, was sufficient to accurately model any continuous function provided a sufficient number of hidden neurons are used. Therefore, this network architecture was chosen for our work. In a fully connected network, each neuron receives inputs from all of the elements in the preceding layer. No connections exist between neurons in the same layer. Figure 6 shows the connection paths to and from one hidden layer neuron. The total input to the hidden layer neuron *j*, U_j , is the summation of the weight multiplied by the input value, x_i , for each connection path.

$$U_j = W_{j0} + \sum_{i=1}^N W_{ji} \times x_i \tag{1}$$

where *N* is the number of inputs, and W_{j0} is the bias of the neuron, which is simply another weight in the network. The bias allows the neuron to have an extra degree of freedom to adjust allowing the input-output relationship to be learned accurately during training.

The output from the hidden layer neuron, V_j , is given by:

$$V_j = f(U_j) \tag{2}$$

where *f* is the activation function. Hornik et al. [29] also showed for the hidden neurons that a sigmoidal activation function, or any other continuous, monotonically increasing, and bounded activation function, is necessary to model the continuous output func-

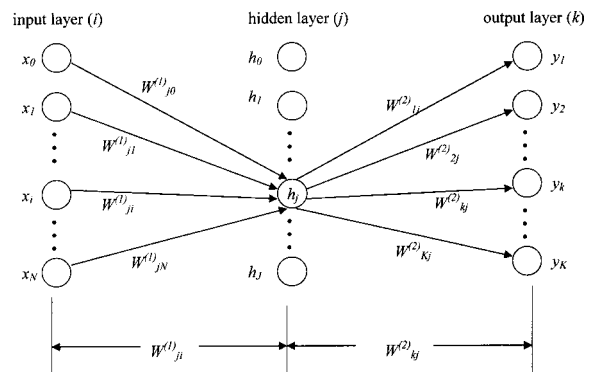


Fig. 6 Structure of neural network

Table 2 HBF and PD% values used to train the network

High Binder Force (kN) Friction Conditions				
Material	No lubricant	Mineral Oil	Prelubricant	Synthetic
CRDSTB	231	280	264	263
EGCR3	(290)	316	312	295
EGCR3-2	163	224	167	(210)
HDGCR3	254	279.5	(268.5)	258
HSGS25S	323	(333.5)	326	326

PD% of total punch displacement Friction Conditions				
Material	No lubricant	Mineral Oil	Prelubricant	Synthetic
CRDSTB	62.35	62.975	61.125	67.5
EGCR3	(61.5)	63.0	61.5	66.0
EGCR3-2	64.0	64.0	67.075	(65.75)
HDGCR3	62.25	63.75	(63.0)	62.75
HSGS25S	61.3	(60.5)	64.0	60.825

*Numbers in parenthesis are those sets used for validation.

tion. However, a simple linear activation function with a slope of one is sufficient for the output neurons. With these two activation functions, a given output, y_k , based on the inputs, x_i , and the connection weights is given by:

$$y_k = \sum_{j=1}^J \left\{ W_{kjo} + W_{kjf} \left(W_{jio} + \sum_{i=1}^N W_{ji} x_i \right) \right\} \quad (3)$$

where J is the total number of hidden neurons.

As was stated above, neural networks must first be trained so they are able to generalize; i.e., to extract, the correct relationship from a finite number of corresponding input-output pairs. During training, a number of input-output pairs, Q , are given to the network and the weights of the connection paths are adjusted. The goal of this “learning” is to get the outputs, y_k , that are calculated using the weights of the neural network as close as possible to the desired output patterns, d_k , for the training examples. A measure of how well the neural network achieves this goal is the Mean Square Error of the process given by:

$$MSE = \frac{1}{Q \times K} \times \sum_{q=1}^Q \sum_{k=1}^K [d_k(q) - y_k(q)]^2 \quad (4)$$

where K is the total number of outputs.

The most common method to adjust the weights of the connection paths is through the back-propagation algorithm [30]. The weights are given a quasi-random, intelligently chosen initial value. Then, the training examples are presented to the neural network one at a time. First, an input pattern, \mathbf{X}_q , is feedforward through the network using the current weights associated with each connection to obtain the output pattern, \mathbf{Y}_q . The capitalized, bold letters represent a vector of input or output values for the current example. From the desired outputs, \mathbf{D}_q , of the training example, errors are computed. Next, the effects of the errors are swept backwards through the neural network to obtain a “square error derivative,” δ , for each computational neuron. A gradient is then calculated for all of the square error derivatives allowing for the weights to be updated. The negative of this gradient represents the direction in which the weights should be adjusted to minimize the MSE of the computations. This process is repeated for all of the training examples and for the specified number of iterations. The number of iterations refers to the number of times that this adjusting procedure is replicated on all of the training examples. The equation for calculating the updated weights is:

$$W^{t+1} = W^t + 2\eta \delta X \quad (5)$$

where η is the learning rate which controls the stability and rate of convergence of the weights. Details for the derivation of this equation are given in Widrow and Lehr [31].

Training Data. The first step to implement a neural network is to generate the training data. For our research, experiments were conducted with stepped binder force trajectories implemented. The desired springback angle range was set to between 10 and 12 deg. This range was chosen based on the capacity of our hydraulic press, i.e., a higher binder force value would be required in order to reduce the springback angle further. The channel forming was done on a particular steel blank using a calculated guess for the HBF and PD% based on simulation results to produce an acceptable springback level. After the stamping operation was completed, the part was removed from the die, and the springback was measured using a Coordinate Measuring Machine (CMM). The strain levels were determined by measuring the deformation of the circle grids on the channel. The process was repeated and iterated by adjusting the HBF and PD% through a trial and error process to obtain acceptable levels of springback angle and strain. When a lubricant was used, care was taken to wipe the punch and binder plate of excess fluid to ensure that each part was formed under the desired friction condition. Once the springback objective was achieved, the experiment was repeated four times in order to ensure reproducibility of the springback angle, strain values, and input parameters calculated by curve fitting the punch force trajectory, which will be discussed in the following paragraph. The springback angle and strain values varied by 0.5 deg and 2% respectively, during the successive process runs. Averaged values of these four tests were regarded as one training set. A total of 20 training sets were generated, a combination of five materials with four lubricant conditions. See Table 2 for a list of all the training data, and Table 3 for the obtained springback angles.

As in Kinsey et al. [18], curve fitting of the punch force trajec-

Table 3 Resultant springback angles for the training data

Springback angles (degrees)				
Material	No lubricant	Mineral Oil	Prelubricant	Synthetic
CRDSTB	10.513	10.347	10.679	10.875
EGCR3	(11.234)	11.098	12.001	11.965
EGCR3-2	11.001	10.789	10.453	(10.791)
HDGCR3	11.3	10.989	(11.351)	11.483
HSGS25S	10.681	(11.504)	12.907	11.339

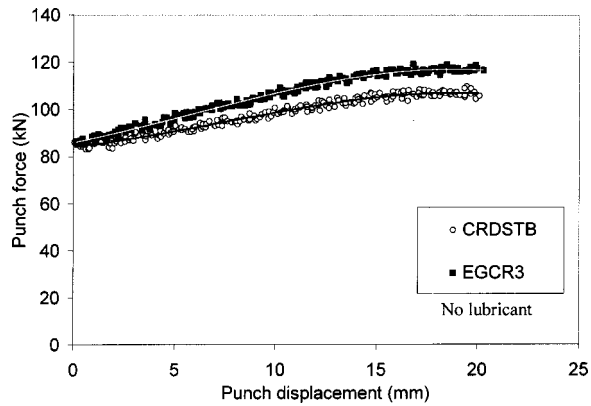


Fig. 7 Punch force trajectories before 20 mm for different materials

tory of the initial forming depth stage of the process was used to determine inputs into the neural network. In post processing of the punch trajectory, it was observed that a third degree polynomial curve fit was able to differentiate between the different materials (see Fig. 7), thicknesses and friction conditions (see Fig. 8) for the values of punch displacement from 0 to 20 mm. The value of 20 mm was determined as the cut off value to calculate the input parameters, because the punch force trajectory reached a constant value at this point. The third degree polynomial curve fitting of the punch force trajectory yielded four coefficients; however, the intercept term was ignored since it was nearly the same for all the cases. Thus, three coefficient terms were used as input parameters to the neural network. During the reproducibility tests, the input parameters varied by a maximum of 6.25%, 7.3%, and 6.9% with respect to the coefficients a , b , and c reported in Table 4.

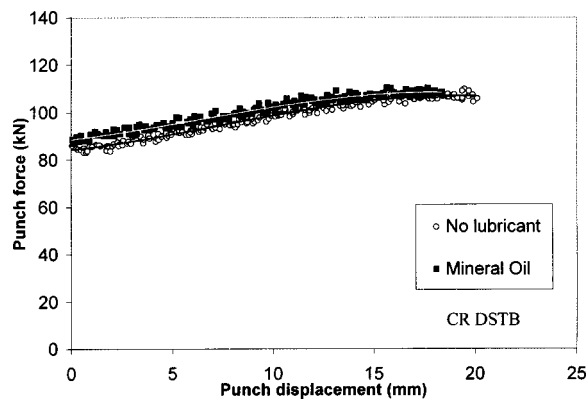


Fig. 8 Punch force trajectories before 20 mm for different friction conditions

Network Establishment. The neural network programming was achieved using the MATLAB Neural Network toolbox. A two-layer neural network was used with a sigmoidal activation function between the input and hidden layers and a linear activation function between the hidden and output layers, as suggested by Hornik et al. [29]. To determine the optimal number of hidden neurons to use in the neural network, a validation study was conducted. First, the training data was separated into two groups of data, a set of sixteen input-output pairs for initially training the neural network and a set of four examples for validation of the training process. These four training input-output pairs are shown in parenthesis and italicized in Tables 2 and 3. The validation study procedure is as follows: First, neural networks with varying numbers of hidden neurons are trained with the sixteen input-output pairs. Then, the inputs from the four validation examples are “feedforward,” i.e., the trained neural network is exposed to the input values, to obtain outputs. Mean square errors are then calculated based on the difference in the output values calculated by the network and the known output data for the four validation examples. With too few hidden layer neurons, the input-output relationship would not be learned adequately leading to a high mean square error. With too many hidden layer neurons, the neural network would be oversensitive and not adapt well to new inputs not seen during training, also leading to high mean square error. For our network, three hidden neurons were determined to be optimal to balance these two conflicting constraints. For more details, refer to Viswanathan [25].

Now that the structure for our neural network was established, i.e., three inputs, three hidden layers, and two outputs, our neural network was retrained with all twenty input and output pairs. The weights and biases were then extracted from the MATLAB neural network software and reconstructed using algebraic equations in our Labview process control program.

Experimental Results

With our neural network calculations now embedded in our Labview process control program, experiments utilizing the control scheme of Fig. 3 were implemented. Various materials with different friction conditions were formed. Curve fitting of the punch force trajectory was performed after 20 mm of forming, and three inputs from this curve fitting were then used as inputs in the neural network equations to determine the HBF and PD% for controlling the springback angle. The neural network was able to determine the stepped binder force trajectory to keep springback within a reasonable range when faced with the same material and friction conditions used to train the network (see Table 5). This verifies that the neural network learned the relationship of the training data well. However, in order to show that the generalized relationship between springback angle and material and process parameters is captured in the neural network, types of steel and friction condition not seen by the neural network during training were also formed. When a generic steel was formed with no lubricant, a EG250B steel with a synthetic lubrication and EGCR3 and HDGCR3 with excessive mineral oil applied, 20 ml., the neural network predicted reasonable values of HBF and PD% to

Table 4 Curve fitting coefficients of punch force trajectory for training the network

Material	Curve fitting coefficients ax^3+bx^2+cx+d , a , b & c											
	No lubricant			Mineral Oil			Prelubricant			Synthetic		
	a	b	c	a	b	c	a	b	c	a	b	c
CRDSTB	-4.1	9.1	10.5	-3.3	7.8	7.5	-3.4	7.2	10.1	-3.2	7.02	8.53
EGCR3	-3.5	8.22	8.39	-3.1	6.79	8.46	-2.9	5.74	10.2	-2.8	5.94	8.68
EGCR3-2	-5.5	10.7	17.0	-3.9	6.86	16	-4.9	9.00	17.3	-4.6	11.5	9.75
HDGCR3	-4.1	8.50	11.8	-3.8	8.25	10.9	-3.8	8.36	10.4	-3.7	8.72	9.26
HSGS25S	-3.6	8.17	11.6	-4.2	9.32	10.4	-3.6	9.20	10.5	-3.7	8.56	7.80

Table 5 Results of experiments with neural network control implemented¹

Material	Friction	Predicted HBF (kN)	Predicted PD%	Springback angle (deg)	Strain (%)
Combinations seen by the network during training					
CRDSTB	No lubricant	247	64.0	10.523	13
EGCR3	No lubricant	290	63.0	11.019	15
EGCR3-2	No lubricant	181	69.1	10.578	14
HDGCR3	No lubricant	256	61.0	11.531	13
HSGS25S	No lubricant	309	59.8	10.809	17
CRDSTB	Mineral Oil	291	65.1	11.179	11
EGCR3	Mineral Oil	311	68.9	10.468	13
HSGS25S	Synthetic	312	61.6	10.259	14.5
Combinations not seen by the network					
HDGCR3	Excess Mineral Oil	304	58.9	10.163	10.5
EGCR3-2	Excess Mineral Oil	248	63.8	10.103	11
EG250B	Synthetic	329	58.9	13.670	10.5
Generic Steel	No lubricant	246	65.2	12.53	9.5

¹Notice that the target springback angle is between 10 to 12 deg.

produce springback only slightly outside the desired range (see Table 5). If these materials and friction conditions were used in the training process as well, better results would have been obtained.

Without the neural network, the springback for the various material and friction conditions in our experiments varied from 4 deg to 30 deg for the same range of binder forces, 160 kN to 330 kN. The CPU was able to perform the neural network calculations fast enough to change to the HBF at the specified PD%. The time required to calculate the outputs of the neural network was 5 milli-seconds on our 233 Hz Pentium microprocessor. The network also provided good results, when the tooling was disassembled and reassembled. This was done to demonstrate that the network could be used in industry where there are frequent tooling changeovers.

Conclusions

Springback control is one of the key concerns of the sheet metal forming industry. The current trial-and-error method of testing and controlling for springback is costly, time consuming, and remains as an obstacle in achieving shorter design and production cycles. Furthermore, unavoidable variations in material and process parameters, which leads to springback uncertainty, require active process control in order to produce consistent parts.

In this paper, a neural network control system along with a stepped binder force trajectory was used to control the springback angle in a steel channel forming process. The neural network control algorithm is able to effectively capture the non-linear relationships and interactions of the process parameters. Three coefficients from a polynomial curve fitting of the punch force trajectory were used as inputs into the neural network, and the outputs were parameters for the stepped binder force trajectory. The results indicate that a neural network of one hidden layer with three neurons was successful in controlling the springback angle between 10° and 12° when faced with sizeable variations in the material properties (20% in K and 27% in n), thicknesses (0.70 to 0.85 mm) and lubricating conditions (0.05 to 0.20). Four different combinations of steel and lubricant condition, which were not used to train the neural network, were formed to demonstrate the ability of our neural network to control the springback angle in general cases. Again reasonable springback angles were obtained (10 to 14 deg). This work demonstrates the benefits of using neural networks to control springback in sheet metal forming. The steel channel forming process was reasonably immune to inevitable variations in process and material parameters thus producing more consistent sheet metal products. It is believed that neural network control will be effective in dealing with material varia-

tions in other sheet metal forming processes. For a complex part forming, punch force alone may not be sufficient in identifying various variations. In these cases, more sophisticated sensors are needed, for example, local draw-in measurement or local tangential force measurement. With these sensors, neural network control combined with real-time closed loop control can dramatically increase the robustness of forming processes.

Acknowledgments

This research was funded by NSF Grant DMI-9703249 and the Engineering Research Program at the Department of Energy. Material and tooling support from U.S. Steel Inc. and ALCOA is deeply appreciated.

References

- [1] "Taking on the "Springback" Challenge," 1995, United States Council for Automotive Research, fall newsletter.
- [2] Karafilis, A. P., and Boyce, M. C., 1996, "Tooling and Binder Design for Sheet Metal Forming Compensating Springback Error," *Int. J. Mach. Tools Manuf.*, **36**(4), pp. 503–526.
- [3] Ghouati, O., Joannic, D., and Genlin, J. C., 1998, "Optimization of Process Parameters for the Control of Springback in Deep Drawing," NUMIFORM'98: Sixth International Conference on Numerical Methods in Industrial Forming Processes, Enschede, Netherlands, June 1998.
- [4] Davies, R. G., and Liu, Y. C., 1984, "Control of Springback in a Flanging Operation," *Journal of Applied Metalwork*, **3**(2), pp. 142–147.
- [5] Marron, G., and Bouhelier, C., 1995, "Bending of High Strength Steels. Prediction and Control of Springback," *Revue de Metallurgie, Cahiers d'Informations Techniques (France)*, **92**(1), pp. 121–130.
- [6] Tarau, M., Teodorescu, M., and Rusu, C., 1997, "Researches Regarding the Influence of Some Technological Factors Toward the Elastic Springback of Some Aluminum Alloys," *Annals of "Dunarea de Jos" University of Galati (Romania)*, **15**, Fascicula V, Technologies in Machine Building, pp. 27–30.
- [7] Song, N., Qian, D., Cao, J., Liu, W., Viswanathan, V., and Li, S. F., 2001, "Effective Models for Prediction of Springback in Flanging," *ASME J. Engrg. Mat. and Tech.*, **123**, pp. 456–461.
- [8] Hu, Y., and Walters, G. N., 1999, "A Few Issues On Accuracy of Springback Simulation of Automobile Parts," SAE Paper No. 1999-01-1000, SAE SP-1435.
- [9] Shi, M. F., and Zhang, L., 1999 "Issues Concerning Material Constitutive Laws and Parameters in Springback," SAE Paper No. 1999-01-1002, SAE SP-1435.
- [10] Zhang, Z. T., Monette, D. G., Monroe, R. J., and Dailey, B. L., 1999 "Establishment of Stamping Process Windows," SAE Paper No. 1999-01-0687, SAE SP-1435.
- [11] Esche, S., and Kinzel, G., 1998, "The Effect of Modeling Parameters and Bending on Two-Dimensional Sheet Metal Forming Simulation," *Adv. Ceram.*, **107**(7), pp. 74–85.
- [12] Li, K., and Wagoner, R. H., 1998, "Simulation of Springback," *Proceedings of Numiform '98*.
- [13] Saran, M. J., and Demeri, M. Y., 1998, "Sensitivity of Forming Process to Selection of Variable Restraining Force Trajectory," SAE Paper No. 982275, SAE SP-334.

- [14] Stein, J. J., 1998, "The Effect of Process Variables on Sheet Metal Springback," SAE Paper No. 982299, SAE SP-334.
- [15] He, N., and Wagoner, R. H., 1996, "Springback Simulation in Sheet Metal Forming," Proceedings of Numisheet '96, pp. 308–15.
- [16] Sunseri, M., Cao, J., Karafillis, A. P., and Boyce, M. C., 1996, "Accommodation of Springback Error in Channel Forming Using Active Binder Force Control: Numerical Simulations and Results," J. Eng. Mater. Technol., **118**(3), pp. 426–35.
- [17] Elkins, K. L., and Sturges, R. H., 1999, "Springback Analysis and Control in Small Radius Air Bending," J. Manuf. Sci. Eng., **121**(4), pp. 679–688.
- [18] Kinsey, B., Cao, J., and Solla, S., 2000, "Consistent and Minimal Springback Using a Stepped Binder Force Trajectory and Neural Network Control," J. Eng. Mater. Technol., **122**, pp. 113–118.
- [19] Dunston, S., Ranjithan, S., and Bernold, E., 1996, "Neural Network Model for the Automated Control of Springback in Rebars," IEEE Expert/Intelligent Systems & Their Applications, **11**(4), pp. 45–49.
- [20] Inamdar, M., Date, P. P., Narasimhan, K., Maiti, S. K., and Singh, U. P., 2000, "Development of an Artificial Neural Network to Predict Springback in Air Vee Bending," International Journal of Advanced Manufacturing Technology, **16**(5), pp. 376–381.
- [21] Kim, D. J., and Kim, B. M., 1999, "Application of Neural Network and FEM for Metal Forming Processes," Int. J. Mach. Tools Manuf., **40**(6), pp. 911–925.
- [22] Manabe, K., Yang, M., and Yoshihara, S., 1998, "Artificial Intelligence Identification of Process Parameters and Adaptive Control System for Deep-Drawing Process," J. Mater. Process. Technol., **80–81**(1), pp. 421–426.
- [23] Ruffini, R., and Cao, J., 1998, "Using Neural Network for Springback Minimization in a Channel Forming Process," Developments in Sheet Metal Stamping, SAE Paper 98M-154, SP-1322, pp. 77–85.
- [24] ABAQUS, 1998, *User's Manual, Theory Manual*, Version 5.8, Hibbit, Karlsson, and Sorensen, Providence, RI.
- [25] Viswanathan, V., 2000, "Physical Implementation of Neural Network for Springback Control," M. S. thesis, Northwestern University, Evanston, IL.
- [26] Sejnowski, T. J., and Rosenberg, C. R., 1986, "Nettalk: A Parallel Network that Learns to Read Aloud," Technical Report John Hopkins University, JHU/EECS-86/01.
- [27] Vitek, J. M., 1999, "Neural Networks Applied to Welding: Two Examples," ISIJ Int., **39**(10), pp. 1088–1095.
- [28] Bounds, D. G., Lloyd, P. J., Matthew, B., and Waddel, G., 1988, "A Multilayer Perceptron Network for the Diagnosis of Low Back Pain," Proceedings of 2nd IEEE International Conference on Neural Networks, San Diego, CA, **2**, pp. 481–489.
- [29] Hornik, K., Stinchcombe, M., and White, H., 1989, "Multilayer Feedforward Networks are Universal Approximators," Neural Networks, **2**, pp. 359–366.
- [30] Rumelhart, D. E., and McClelland, J. L., 1986, "Learning Internal Representation by Error Propagation," *Parallel Distributed Processing*, MIT Press, Cambridge, MA, **1**, Chap. 8.
- [31] Widrow, B., and Lher, M. A., 1990, "30 Years of Adaptive Neural Networks: Perceptron, Madaline and Backpropagation," Proceedings of the IEEE, **78**, (9), pp. 1415–1441.